Separation Science and Technology
Publication details, including instructions for authors and subscription information:
http://www.informaworld.com/smpp/title~content=t713708471

Semicontinuous pH Parametric Pumping: Process Characteristics and Protein Separations

H. T. Chen[a]; W. T. Yang[a]; C. M. Wu[a]; C. O. Kerobo[a]; V. Jajalla[a]
[a] DEPARTMENT OF CHEMICAL, ENGINEERING NEW JERSEY INSTITUTE OF TECHNOLOGY, NEWARK, NEW JERSEY

To cite this Article Chen, H. T. , Yang, W. T. , Wu, C. M. , Kerobo, C. O. and Jajalla, V.(1981) 'Semicontinuous pH Parametric Pumping: Process Characteristics and Protein Separations', Separation Science and Technology, 16: 1, 43 — 61
To link to this Article: DOI: 10.1080/01496398108070224
URL: http://dx.doi.org/10.1080/01496398108070224

SEPARATION SCIENCE AND TECHNOLOGY, 16(1), pp. 43-61, 1981

Semicontinuous pH Parametric Pumping: Process Characteristics and Protein Separations

H. T. CHEN,* W. T. YANG, C. M. WU,
C. O. KEROBO, and V. JAJALLA

DEPARTMENT OF CHEMICAL ENGINEERING
NEW JERSEY INSTITUTE OF TECHNOLOGY
NEWARK, NEW JERSEY 07102

Abstract

A semicontinuous pH parametric pump was experimentally and theoretically investigated using the model system of hemoglobin–albumin–CM Sepharose. A mathematical model with finite mass transfer was developed, and agrees quite well with experimental data. Various factors affecting separations were examined. It is shown that under certain operating conditions, the continuous process can be operated with large feed throughput and with high separation factors.

INTRODUCTION

pH parametric pumping is a cyclic separation process which involves reciprocating flow of a fluid phase over a solid phase in a packed bed and at the same time synchronous periodic variation of pH. Very little work has been done on pH parapumps. Sabadell and Sweed (*6*) used pH changes to concentrate aqueous solutions of K^+ and Na^+. Shaffer and Hamrin (*7*) studied trypsin concentration by affinity chromatography and parametric pumping.

Chen et al. (*2, 3*) have studied the separation of hemoglobin and albumin by one-column pH parametric pumping. The experimental data have shown that a pH driven parapump is capable of yielding very high separation factors. Most recently, Chen et al. (*4*) indicated that the multicolumn parapump (columns packed alternately with cation and anion exchangers) has much higher separation capability than the one-

*To whom correspondence should be addressed.

column unit. Furthermore, a simple graphical method based on an equilibrium theory was presented to show how the separation builds from cycle to cycle, and to give a better understanding of the origin of separation. In this paper a mathematical model with finite mass transfer is presented. The pH pump considered is a semicontinuous mode. Computer simulations are made for a wide range of operating conditions. Emphasis is placed on the conditions necessary to achieve desired separations.

PROCESS DESCRIPTION

The pump we have studied is shown in Fig. 1. It consists of a column packed with an ion exchanger (cation or anion) and reservoirs attached to each end. The pump has dead volumes V_T and V_B for the top and bottom reservoirs, respectively. Initially, the mixture to be separated fills the column voids, the top reservoir, and bottom dead volume. The top reservoir is maintained at a low pH level (P_2) by an automatic titrator while a second titrator is used to keep the bottom reservoir at a high pH level (P_1). The buffer ionic strengths for the solutions to the bottom and top of the column are kept at IS_1 and IS_2, respectively, by means of two hollow fiber dialyzers. In a previous paper (*3*) we have shown that a desired protein A can be separated from a mixture provided that its isoelectric point I_A lies between the two pH levels, i.e., $P_2 < I_A < P_1$.

The flow system has eight distinct steps in each cycle (Fig. 1):

I. Pump the low pH (P_2) fluid from the top reservoir to the top of the column for time t_I while the solution emerging from the other end enters the bottom reservoir.

II. Circulate the fluid between the top reservoir and the column for time t_{II}. During this stage the pH in the column is ensured to change from P_1 to P_2. As a result, S^+ is exchanged for the A^+ originated from the top reservoir.

III. Feed at the bottom of the column with the mixture of pH = P_2 for time t_{III}, and simultaneously a top product free of A is removed from the column at the same rate. In addition, the A^+ initially present in the bottom feed is exchanged for S^+.

IV. Circulate the fluid between the top reservoir and the column for time t_{IV}. This will allow the concentration in the column and the top reservoir to become uniform.

V. Pump the fluid with pH = P_1 from the bottom reservoir to the bottom of the column for time t_V, and at the same time the solution free of protein A flows out of the column to the top reservoir.

VI. Circulate the fluid between the bottom reservoir and the column for time t_{VI}. This will ensure that the pH in the column is shifted back to

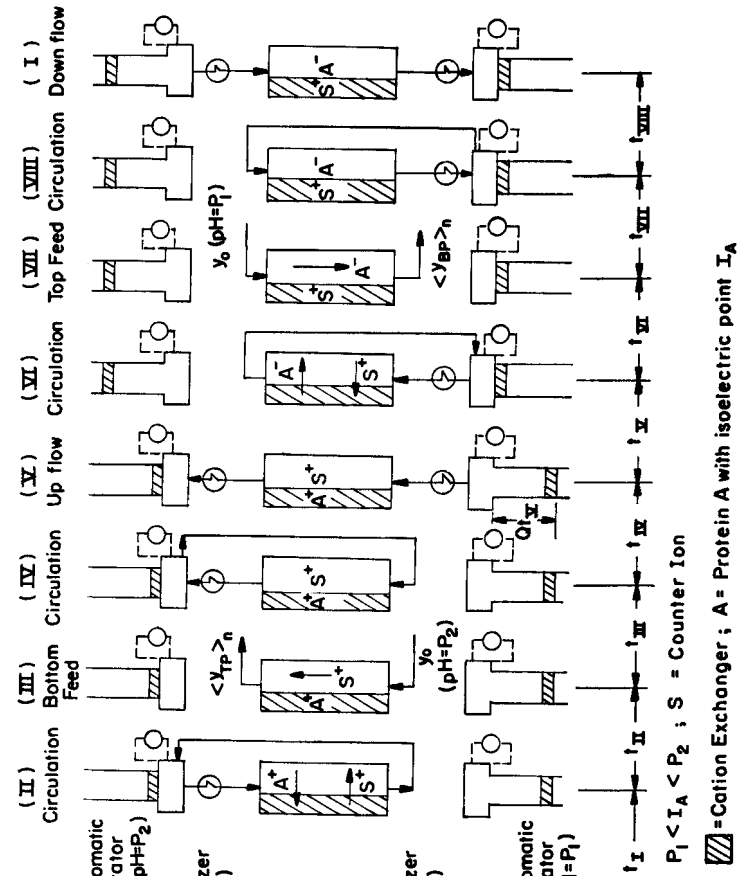

FIG. 1. Column diagram for semicontinuous pH parametric pumping.

P_1 and desorption of A occurs. S^+ shifts back to the bed and the ion exchanger is then regenerated.

VII. Feed at the top with the mixture of pH = P_1 for time t_{VII}, while a product rich in A is withdrawn from the bottom of the column.

VIII. Circulate the fluid between the column and the bottom reservoir. This will result in a uniform concentration between the column and the bottom reservoir. One whole cycle is thus completed.

By repeating the process described above in the succeeding cycles, in the limit of a large number of cycles, the system is capable of removing most of the A from the feed streams and transferring it to the bottom product stream. Note that the flow rate (Q) within the column is always identical to the reservoir displacement rate. The volumes of the bottom and top feed (Qt_{III} and Qt_{VII}) are equal to those of the top and bottom products, respectively. Also, the up- and downflow have the same displacement; that is, $Qt_I = Qt_V$.

MATERIAL BALANCES

Two types of equations are needed in calculating the performance characteristics of the parapump: internal and external equations. An external equation is a solute material balance on streams flowing to and from a reservoir. A detailed description of external equations is shown in a paper by Chen and Hill (*1*).

Internal equations are the solute material balances reflecting the events occurring within the adsorption column. By assuming plug flow, dilute solution, and linear equilibrium adsorption, and neglecting axial diffusion,

$$\varepsilon v\frac{\partial y}{\partial z} + \varepsilon\frac{\partial y}{\partial t} = -(1 - \varepsilon)\frac{\partial x}{\partial t} \tag{1}$$

$$\frac{\partial x}{\partial t} = \lambda(y - y^*) \tag{2}$$

$$y^* = x/k \tag{3}$$

where k is dependent on the buffer pH, ionic strength, and substance (i.e., the components from which the buffer is made). The pH within the bed is in turn a function of position (z) and time (t), and depends on fluid flow rate (Q), ionic strengths (IS_1 and IS_2), and pH levels (P_1 and P_2). Calculations of velocities of the pH and ionic strength waves are very complex and have to be experimentally determined. However, for the present system (hemoglobin–albumin–CM Sepharose in a buffer of monobasic and dibasic phosphate), there is essentially no lag of pH or ionic strength wave velocity behind the linear liquid velocity (*2*, *3*),

$$v_{\text{pH}} = v_{\text{ionic strength}} = v \tag{4}$$

Replace the time and position derivatives in Eq. (1) by the lowest order backward differences:

$$\varepsilon v\Delta t[y(I, J-1) - y(I-1, J-1)] + \varepsilon\Delta z[y(I, J) - y(I, J-1)] = -(1-\varepsilon)\Delta z[x(I, J) - x(I, J-1)] \tag{5}$$

Divide the column into NZ equal position increments, and the time domain into $NT1, NT2, \ldots, NT8$ time increments, respectively, for the stages I, II, ..., VIII (Fig. 1) such that the displacement during each time increment equals the length of one position increment. That is,

$$\frac{h}{NZ} = \Delta Z = v\Delta t = \frac{Qt_{\text{I}}}{A_c(NT1)} = \frac{Qt_{\text{II}}}{A_c(NT2)} = \frac{Qt_{\text{III}}}{A_c(NT3)} = \frac{Qt_{\text{IV}}}{A_c(NT4)} = \frac{Qt_{\text{V}}}{A_c(NT5)} = \frac{Qt_{\text{VI}}}{A_c(NT6)} = \frac{Qt_{\text{VII}}}{A_c(NT7)} = \frac{Qt_{\text{VIII}}}{A_c(NT8)} \tag{6}$$

Hence, Eq. (5) takes the form

$$y(I. J) = y(I-1, J-1) - \left(\frac{1-\varepsilon}{\varepsilon}\right)[x(I, J) - x(I, J-1)] \tag{7}$$

Substituting Eqs. (3) and (7) into (2),

$$\frac{\partial x}{\partial t} = \lambda\left[y(I-1, J-1) + \left(\frac{1-\varepsilon}{\varepsilon}\right)x(I, J-1) - \left(\frac{1-\varepsilon}{\varepsilon}\right)x(I, J) - \frac{1}{k}x(I, J)\right] \tag{8}$$

Integrating Eq. (8) with respect to t over the time increment Δt,

$$x(I, J) = \frac{y(I-1, J-1) + \left(\frac{1-\varepsilon}{\varepsilon}\right)x(I, J-1)}{\left(\frac{1-\varepsilon}{\varepsilon}\right) + \frac{1}{k}} + \left[x(I, J-1) - \frac{y(I-1, J-1) + \left(\frac{1-\varepsilon}{\varepsilon}\right)x(I, J-1)}{\left(\frac{1-\varepsilon}{\varepsilon}\right) + \frac{1}{k}}\right] e^{-\lambda((1-\varepsilon)/\varepsilon + 1/k)\Delta t} \tag{9}$$

From Eqs. (4), (6), (7), and (9), along with the external equations, the concentration transients (i.e., $\langle y_{TP}\rangle_n$ and $\langle y_{BP}\rangle_n$ vs n) can be calculated by the STOP-GO method developed by Sweed and Wilhelm (*8*). Note that as $\lambda \to \infty$, there is an equilibrium between adsorbate in the solid and liquid phases, and by setting $y = y^*$, Eq. (3) can be directly substituted into Eq. (7) for the calculation of transients.

TABLE 1

Experimental and Model Parameters[a]

Run	Q (m^3/s)	t_c (s)	$\lambda \times 60$	F_B (m^3)	F_T (m^3)	$V_T = V_B$ (m^3)	y_{co}/y_o	
							Hemoglobin	Albumin
2	1.667×10^{-8}	1,440	Equilibrium	4×10^{-6}	9×10^{-6}	5×10^{-6}	0.9	1.0
3	1.667×10^{-8}	1,440	Equilibrium	2×10^{-6}	5.5×10^{-6}	5×10^{-6}	0.9	1.0
4	1.667×10^{-8}	0	0.3	5×10^{-6}	6.5×10^{-6}	15×10^{-6}	0.5	1.0
6	1.667×10^{-8}	0	0.3	10×10^{-6}	12×10^{-6}	15×10^{-6}	0.5	1.0
7	3.333×10^{-8}	0	0.19	4×10^{-6}	9×10^{-6}	15×10^{-6}	0.5	1.0
8	5×10^{-8}	0	0.14	3×10^{-6}	9×10^{-6}	15×10^{-6}	0.7	1.0

[a] $k_1 = 0.33$, $P_1 = 8$, $IS_1 = 0.2\ M\ NaH_2PO_4 + 0.2\ M\ Na_2HPO_4 + 0.1\ M$ NaCl. $k_2 = 5$, $P_2 = 6$, $IS_2 = 0.05\ M\ NaH_2PO_4 + 0.05\ M\ Na_2HPO_4$. $L = 0.08$ m, $y_o = 0.02$ wt-% of hemoglobin + 0.02 wt-% of albumin, $Qt_1 = 1.2 \times 10^{-5}\ m^3$.

EXPERIMENTAL

The performance of pH-parametric pumps was studied for the case of hemoglobin–albumin on CM Sepharose. The buffers were mixtures of monobasic and dibasic sodium phosphates. The experimental apparatus used was similar to that used previously (*3*). Table 1 summarizes the experimental conditions for selected experiments, and the data are plotted in Figs. 4 to 7.

The isoelectric points for hemoglobin and albumin are 6.7 and 4.7, respectively. For all runs $P_1 = 8$ and $P_2 = 6$, so the isoelectric point of hemoglobin lies between the two pH levels. This will lead to the result that hemoglobin would be removed from the top product stream and concentrated in the bottom product stream.

Samples taken from the product streams at the end of each cycle were analyzed by using a spectrophotometer (Bausch and Lomb Spectronic

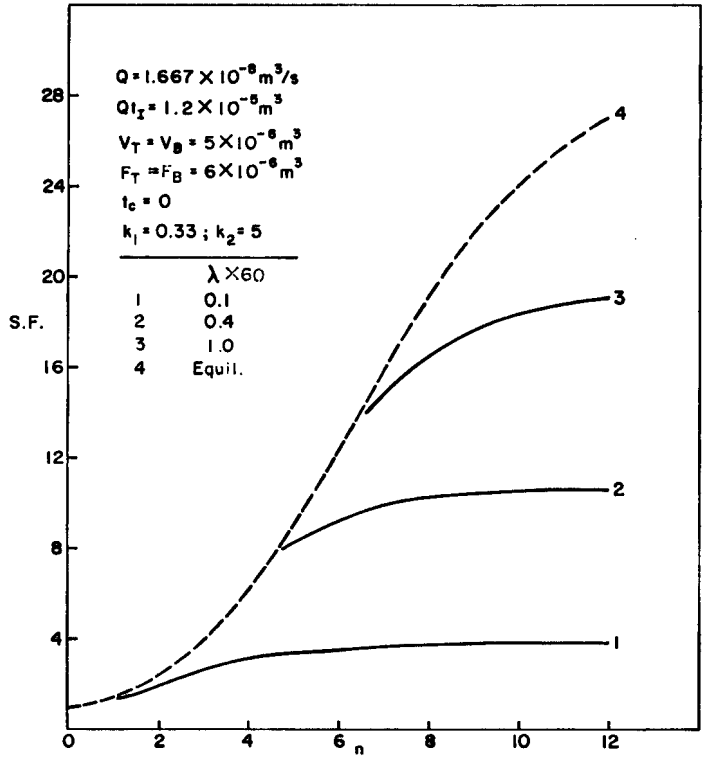

FIG. 2. Effect of λ on separation.

System 400–3). The hemoglobin concentration was determined directly from the absorbance at a wavelength of 403 μm. Bio-Rad protein assay was used to obtain the total protein concentration. Hence subtraction of the hemoglobin concentration from the total gives the concentration of albumin.

DETERMINATION OF EQUILIBRIUM AND RATE CONSTANTS

To implement the computation of concentration profiles, we must have the equilibrium constants k_1 and k_2 and the rate constant λ. These parameters can be determined experimentally via the following modes of pump operation.

Mode 1: No circulation ($t_c = t_{II} = t_{IV} = t_{VI} = t_{VIII} = 0$)

Figure 2 shows the calculated separation factor ($\langle y_{BP}\rangle_n/\langle y_{TP}\rangle_n$) vs number of cycles for several values of λ. As expected, this parameter does significantly affect the separation. For small λ, little transfer occurs between phases and hence little separation takes place. As λ increases,

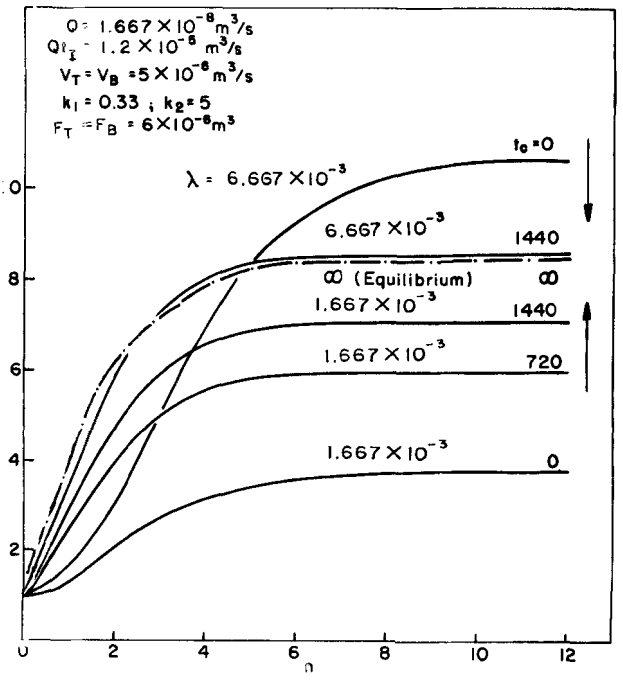

FIG. 3. Effect of t_c on separation. Ordinate: S.F.

the amount of interphase solute transfer increases toward a limit imposed by equilibrium.

Mode 2: With circulation and assume that $t_{II} = t_{IV} = t_{VI} = t_{VIII} = t_c$, where t_c = duration of circulation

Figure 3 shows the calculated separation factors vs n for $\lambda = 1.667 \times 10^{-3}$ and 6.667×10^{-3}. As t_c increases, S.F. will increase or decrease, depending on the value of λ, and approach a limit-equilibrium condition. When the value of λ is small (i.e., 1.667×10^{-3}), S.F. increases with t_c. However, for a larger value of λ (i.e., 6.667×10^{-3}), an opposite effect will result. Also, as t_c increases, the mixing between the column and reservoir becomes significant, and at the end of each circulation step

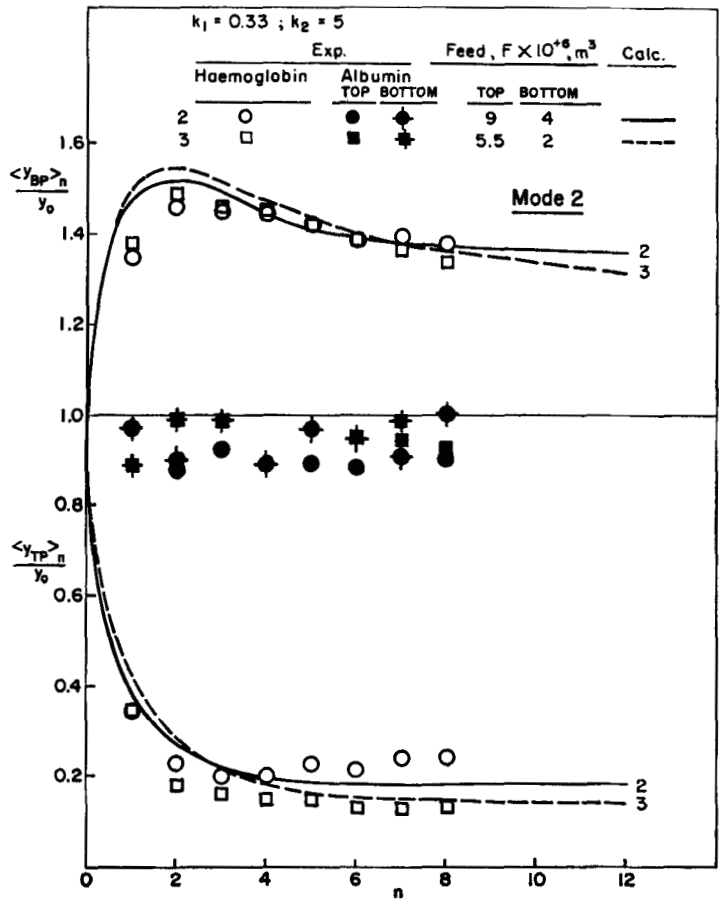

FIG. 4. Experimental and calculated concentration transients.

[i.e., Steps II, IV, VI, or VIII (Fig. 1)] the adsorption column should have a uniform concentration in either fluid or solid phase.

Figures 4 and 5 show the typical experimental results by Modes 2 and 1, respectively. As expected, hemoglobin does migrate downward and accumulate at the bottom end. In both top and bottom product streams, albumin concentration is essentially unaffected.

The experimental data shown in Fig. 4 were obtained based on t_c = 1440 s. Although not shown, the results for $t_c > 1440$ s are essentially identical to those for $t_c = 1440$ s. This is to say that the data shown in Fig. 4 were obtained at an equilibrium. These data were used to predict the equilibrium constants as follows: (1) assume values of k_1 and k_2,

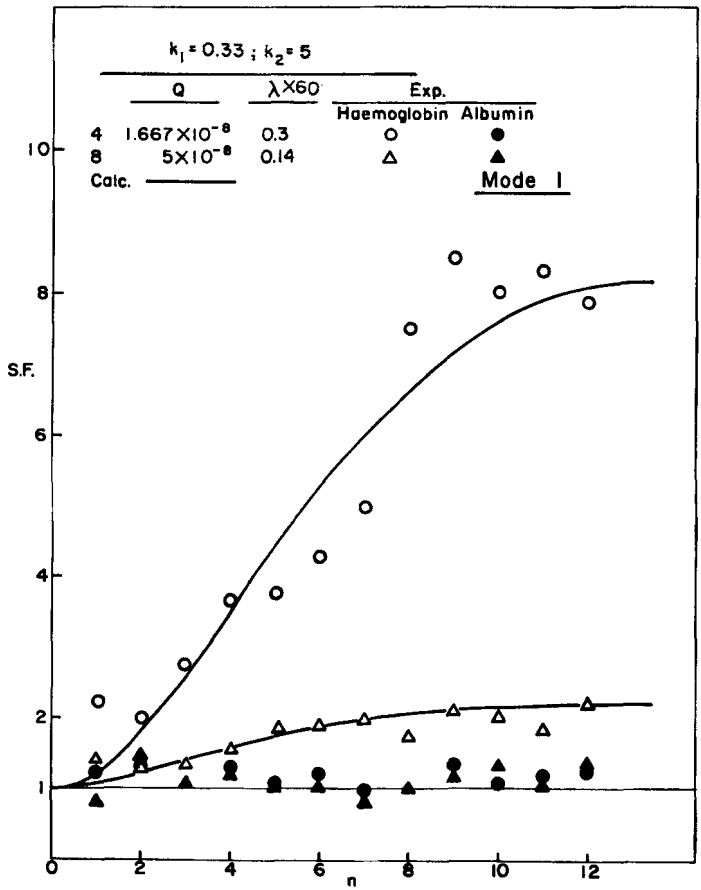

FIG. 5. Experimental and calculated separation factors.

(2) let $\lambda \to \infty$ and calculate the transients using the STOP-GO method, and (3) if the calculated results fit with the data, k_1 and k_2 are the desired values. If not, assume new equilibrium constants and repeat Steps 2 and 3. The estimated values of k_1 and k_2 for Runs 2 and 3 (Fig. 4) are $k_1 = 0.33$ and $k_2 = 5$, respectively.

Figure 5 shows the experimental results via Mode 1 for $Q = 1.667 \times 10^{-8}$ and 5×10^{-8} m^3/s. The data were used to determine the velocity dependence of λ. The values of λ were obtained by matching calculated plots of separation factor vs n with experimental data using the following procedures: (1) assume the value of λ, (2) using the k values obtained above, calculate the S.F. vs n (by the STOP-GO method), and (3) if the calculated results check with the data, the λ is the desired one. If not, assume a new λ and repeat Steps 2 and 3.

The estimated λ's for Runs 4 and 8 are:

$$\text{Run 4: } \lambda_1 = 5 \times 10^{-3} \text{ for } Q_1 = 1.667 \times 10^{-8}$$

$$\text{Run 8: } \lambda_2 = 2.33 \times 10^{-3} \text{ for } Q_2 = 5 \times 10^{-8}$$

By applying (*8*, *9*),

$$\left(\frac{\lambda_2}{\lambda_1}\right) = \left(\frac{Q_1}{Q_2}\right)^a \tag{10}$$

or $a = 0.693$. Thus

$$\lambda = \lambda_1\left(\frac{Q_1}{Q}\right)^a = 2.036 \times 10^{-8} Q^{-0.693} \tag{11}$$

From Eq. (11), one can calculate λ for any given Q. Equation (11) and the estimated k values are based on Runs 4 and 8, and can only be applied to a parapumping system for which the buffer pH levels (P_1 and P_2) and ionic strengths (IS_1 and IS_2) are identical to those for Runs 4 and 8.

RESULTS AND DISCUSSION

Using model equations along with Eq. (11) (expression for λ) and the values of k_1 and k_2, we have successfully simulated parametric pumping separation. It should be pointed out that Eq. (11) is derived from the data of separation factor (S.F.) vs number of cycles (n). It can also be applied to the prediction of concentration transients (Fig. 6). The agreement between calculated results and the data is quite good. Figure 7 shows two additional experimental runs used in verifying the validity of the model.

The effect of Q on separation is also shown in Figs. 6 and 7. A decrease in Q results in an increase in λ, and thus separation. However, if Q becomes

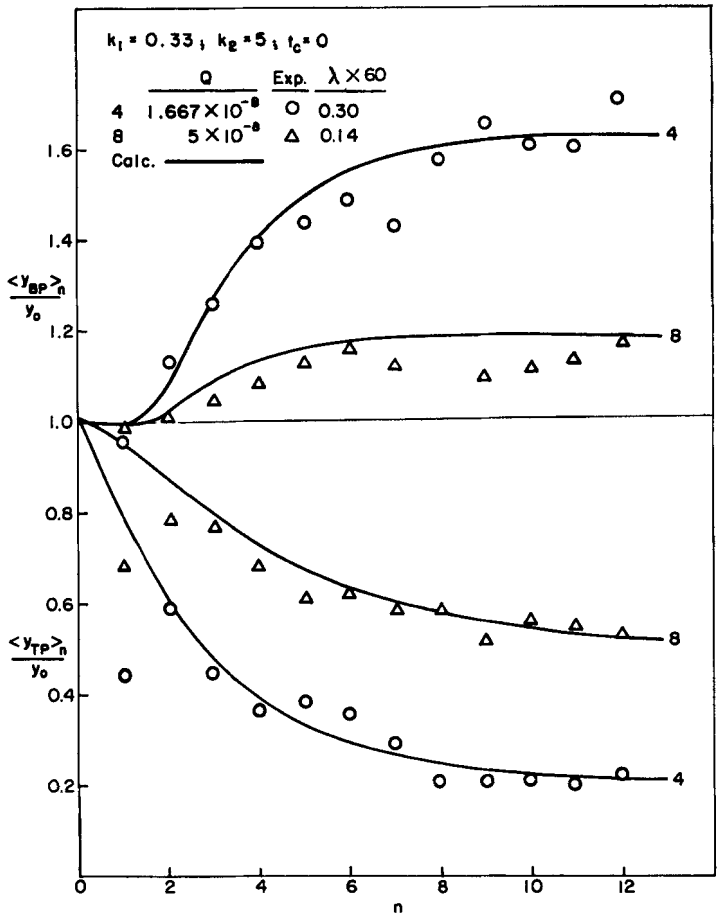

FIG. 6. Comparison of calculated transients with experimental data for Runs 4 and 8.

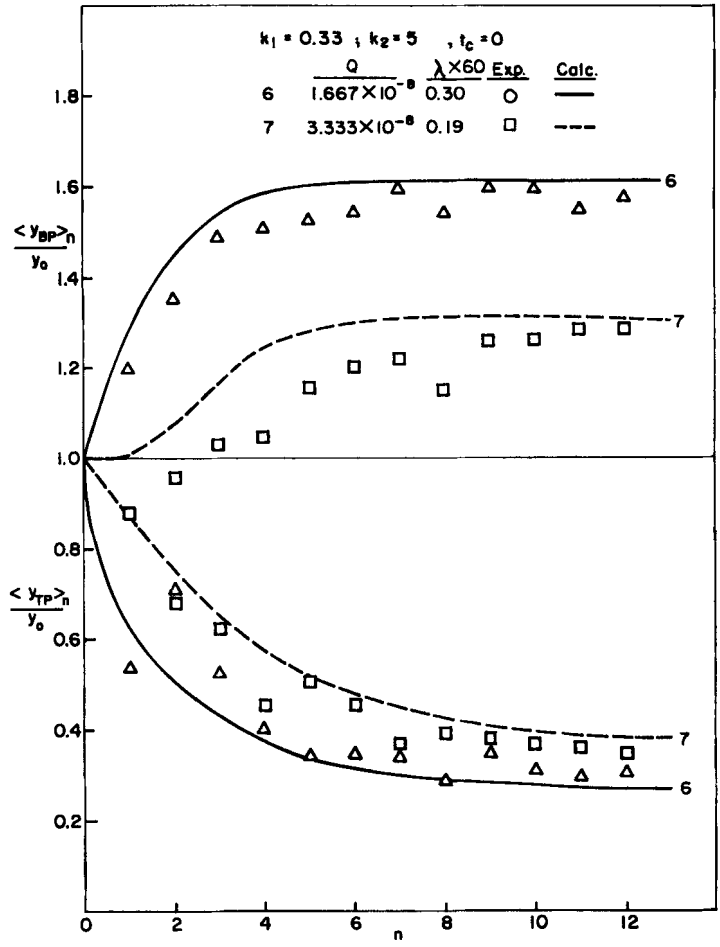

FIG. 7. Comparison of calculated transients with experimental data for Runs 6 and 7.

too small, axial diffusion may become significant, and a poor separation may result.

Figure 8 illustrates the effect of feed on separation. This figure shows the calculated results (for $F_T = F_B$) with $t_c = 0$. F_B and F_T are equal to Qt_{III} (bottom feed) and Qt_{VII} (top feed), respectively. For small λ (i.e., $\lambda = 0.005$), the separation ($(S.F.)_\infty$) decreases as F_T (or F_B) increases. For large λ or a pump operated near equilibrium, an increase in feed increases $(S.F.)_\infty$, very rapidly reaching a maximum value. Further increase in feed results in a drop of $(S.F.)_\infty$ because of the intermixing between the feed and product streams.

Wilhelm et al. (*10*) studied thermal recuperative parapumps and showed that for large values of γ (heat transfer rate constant between the solid and fluid phases) the steady-state separation factor for a batch pump is

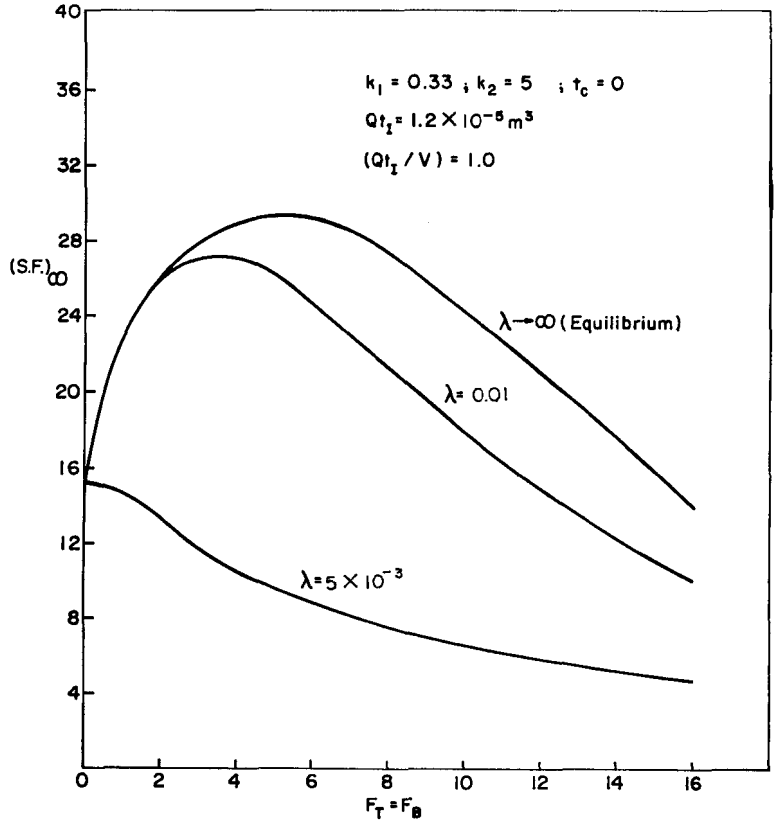

FIG. 8. Effect of feed on separation.

essentially a constant and does not change with λ. This is consistent with what we have shown in Fig. 8. Note that this figure is based on the assumption that there is no lag between the fluid displacement and pH transfer flux (i.e., Eq. 4), corresponding to $\gamma \to \infty$ in Wilhelm's thermal pump. At $F_T = F_B = 0$ (the pump is operated batchwise), the $(\text{S.F.})_\infty$ is 15 and is independent of λ. This occurs because for a batch pump, regardless of λ, compositional equilibrium exists between phases at steady state ($n \to \infty$).

Figure 9 shows the effect of F_T and F_B on the bottom product concentration. The volumes of top and bottom feeds (F_T and F_B) are equal to those for bottom and top products (P_B and P_T), respectively. As F_T decreases or F_B increases, $\langle y_{BP} \rangle_\infty / y_0$ increases. The effect becomes more profound at low values of F_T. If one desires, for example, to obtain a very high concentration of a desired protein from a mixture, one would operate a pump at a low value of F_T and a high value of F_B. Also, for a given $\langle y_{BP} \rangle_\infty / y_0$, an increase in the bottom feed (F_B) results in an increase in the bottom product (P_B).

Figure 10 shows the effect of the column height on the separation. Two cases are considered: $h = 0.08$ and $h = 0.16$ m. The values of Qt_I, F_T, and F_B for $h = 0.16$ m are set to be twice those for $h = 0.08$ m. For

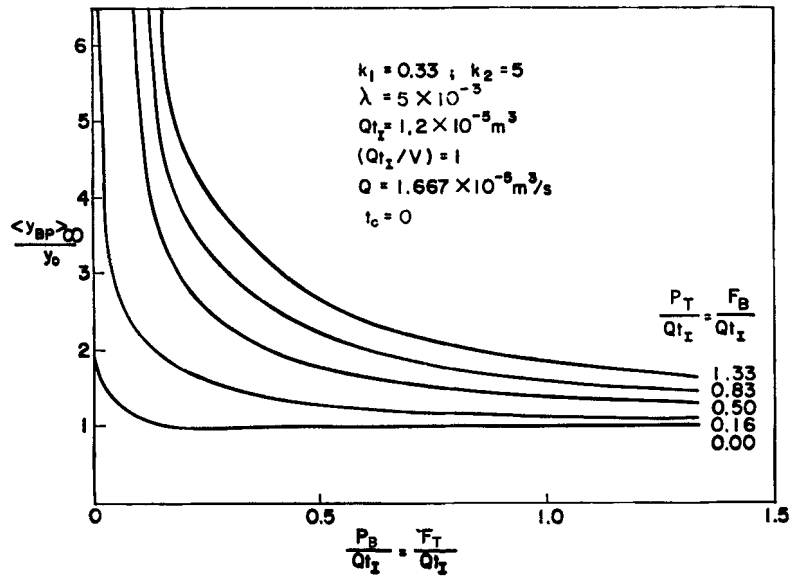

FIG. 9. Effect of feed on the bottom product concentration.

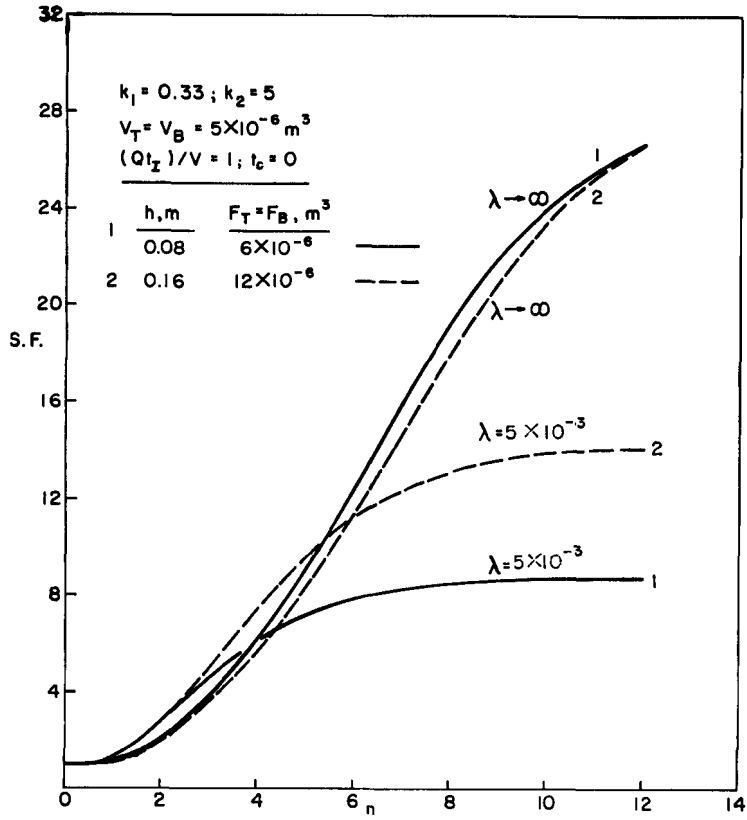

FIG. 10. Effect of column height on separation.

the equilibrium case ($\lambda\to\infty$), h has essentially no effect on the separation. For the case of finite mass transfer, separation increases with h.

The influence of the dead volume (V_T or V_B) in the reservoir is shown in Fig. 11. Increasing the volume shows a decrease in the separation rate but does not affect the ultimate separation.

We present here a simple means of predicting protein separation by pH driven parametric pumping. The good agreement between the experiment and the calculated results indicates that the STOP-GO algorithm developed by Sweed and Wilhelm (*8*) is a useful method for calculating concentration transients for parapumping systems.

CONCLUSIONS

A mathematical model is presented for a semicontinuous pH parapump.

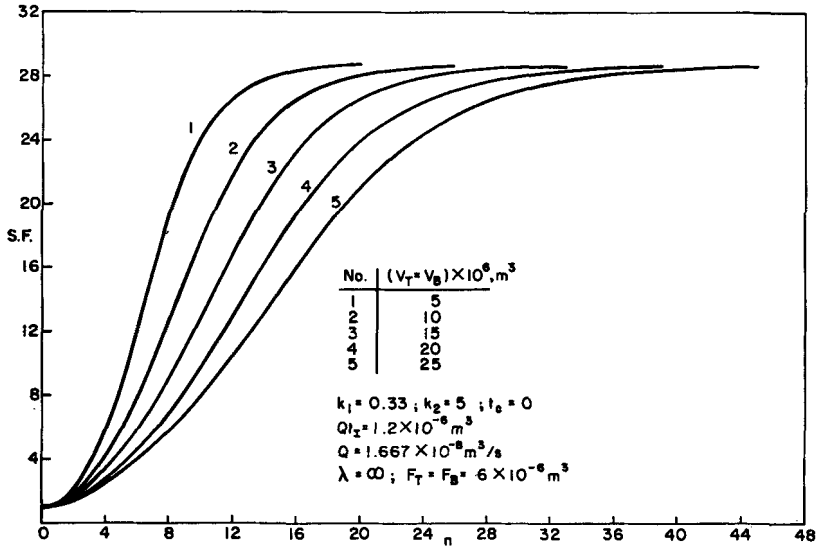

FIG. 11. Effect of dead volume on separation.

The equilibrium and mass transfer rate constants in this model are determined by matching the calculated results with experimental data. The model is shown to simulate experimental systems quite well with various operating conditions.

The parapump system has a feed containing the protein mixture to be separated, introduced alternately to the top and bottom of the chromatographic column. The top and bottom products are withdrawn from the apparatus during the bottom and top feed, respectively. After an initial transient, the product concentrations reach a limiting condition and remain constant as the number of cycles continues to increase. This offers significant advantages over the batch pump. In addition, by proper adjustment of feeds, one can purify a desired protein from a mixture to a desired concentration.

SYMBOLS

A_c	column cross-sectional area (m^2)
F_B	$P_T = Qt_{III}$ = bottom feed
F_T	$P_B = Qt_{VII}$ = top feed
h	column length (m)
I_i	isoelectric point of i
IS_1	ionic strength in the bottom reservoir

IS_2 ionic strength in the top reservoir
k equilibrium constant defined by Eq. (3)
n number of cycles of pump operation
P_B bottom product (m^3)
P_T top product (m^3)
P_1 high pH level
P_2 low pH level
Q reservoir displacement rate (m^3/s)
t time duration (s)
t_c circulation time (s)
V volume of fluid phase per stage (m^3)
$\overline{V}$ volume of solid phase per stage (m^3)
V_B bottom reservoir dead volume (m^3)
V_T top reservoir dead volume (m^3)
x concentration of solute in the solid phase (kg mol/m^3)
y concentration of solute in the fluid phase (kg mol/m^3)
y_{co} initial concentration of solute in the column (kg mol/m^3)
y_o concentration of solute in the feed (kg mol/m^3)
$\langle y_B \rangle_n$ average concentration of solute in the bottom reservoir at nth cycle (kg mol/m^3)
$\langle y_T \rangle_n$ average concentration of solute in the top reservoir at nth cycle (kg mol/m^3)
z position (m)
S.F. separation factor defined as the ratio of the bottom product concentration to the top product concentration (dimensionless)
ε void fraction in packing (dimensionless)
λ mass transfer rate constant as defined by Eq. (2) (l/s)
v linear velocity (m/s)

Subscripts

1 upflow or high pH
2 downflow or low pH
BP bottom product
n *n*th cycle
TP top product
∞ steady state

Acknowledgment

This work was supported by the National Science Foundation under Grants ENG 77–04129 and ENG 79–10540.

REFERENCES

1. H. T. Chen and F. B. Hill, *Sep. Sci.*, *6*, 411 (1971).
2. H. T. Chen, T. K. Hsieh, H. C. Lee, and F. B. Hill, *AIChE J.*, *23*, 695 (1977).
3. H. T. Chen, Y. W. Wong, and J. S. Wu, *Ibid.*, *25*, 320 (1979).
4. H. T. Chen, W. T. Yang, U. Pancharoen, and R. Parisi, *Ibid.*, *26*, 839 (1980).
5. H. T. Chen, U. Pancharoen, W. T. Yang, C. O. Kerobo, and R. Parisi, *Sep. Sci. Technol.*, *15*, 1377 (1980).
6. J. E. Sabadell and N. E. Sweed, *Sep. Sci.*, *5*, 171 (1970).
7. A. G. Shaffer and C. E. Hamrin, *AIChE J.*, *21*, 782 (1975).
8. N. H. Sweed and R. H. Wilhelm, *Ind. Eng. Chem., Fundam.*, *8*, 221 (1969).
9. N. H. Sweed and R. A. Gregory, *AIChE J.*, *17*, 171 (1971).
10. R. H. Wilhelm, A. W. Rice, R. W. Rolke, and N. H. Sweed, *Ind. Eng. Chem., Fundam.*, *7*, 337 (1968).

Received by editor May 23, 1980